ELSEVIER

Materials Science and Engineering A 485 (2008) 681–689

MATERIALS SCIENCE & ENGINEERING A

www.elsevier.com/locate/msea

Effect of strain rate on the compressive mechanical properties of aluminum alloy matrix composite filled with discontinuous carbon fibers

Jing Cai [a], Yuejian Chen [c], Vitali F. Nesterenko [a,b], Marc A. Meyers [a,b,*]

[a] *Materials Science and Engineering Program, University of California, San Diego, CA 92093, United States*
[b] *Department of Mechanical and Aerospace Engineering, University of California, San Diego, CA 92093, United States*
[c] *Metal Matrix Cast Composite, LLC, 101 Clematis Avenue, Waltham, MA 02453, United States*

Received 11 July 2007; received in revised form 15 August 2007; accepted 16 August 2007

Abstract

Compression and forced shear loading were utilized to investigate the quasi-static and dynamic response of carbon fiber/Al–Mg composites. Two types of carbon fibers (PAN-based (C_{PAN}) and pitch-based (C_{Pitch})) were introduced into an Al–Mg alloy matrix (∼30 vol% fibers). The C_{PAN}/Al–Mg composite had higher compressive and shear strengths than C_{Pitch}/Al–Mg regardless of fiber orientation. The difference in strength due to the nature and probably quality of the fibers was more significant than the effect of fiber orientation (perpendicular or parallel to loading direction). The compressive strength of these composites exhibited a strain rate sensitivity comparable with that of an Al–Mg alloy and more pronounced for the C_{PAN}/Al–Mg composite. The microstructural features of shear flow in the localized shear zone in hat-shaped specimens and the characteristics of fractured fibers are analyzed and discussed. Possible reaction of the metal matrix and carbon fibers was observed.

Keywords: Carbon fiber reinforced Al matrix composite; High-strain rate deformation

1. Introduction

Carbon fibers are widely used in composites to tailor strength and modulus and to decrease the density of composites [1–4]. Many studies have focused on the interfacial properties, seeking to improve the bonding between carbon fibers and the matrix [5–7], and on the influence of the carbon fiber content in the composites [8–10]. Recently, some researchers started to pay attention to the dynamic response of carbon fiber reinforced metal matrix composites [11,12].

The present investigation is aimed at: (a) establishing the effect of the carbon fiber (pitch-based and PAN-based (polyacrylonitrile)) on the mechanical response and strain rate sensitivity of a composite with Al–Mg metal matrix and (b) determining the failure evolution mechanism and the effect of the orientation of carbon fibers on the strength of the composites.

The composites being investigated were developed for tailored coefficients of thermal expansion and heat conductivity. The applications are in electronic thermal management, wireless communication systems, heat sinks for phased array radar antennas, and base plate applications for commercial power semiconductors used in hybrid electric vehicles (HEV) and static transfer switching technology. For instance, the addition of 30% graphite fibers decreases the CTE from $24 \times 10^{-6}\,K^{-1}$ to $\sim 8 \times 10^{-6}\,K^{-1}$. The compressive strength of the metal matrix cast composite METGRAF^{TM} is approximately 200 MPa. The manufacturing procedure is described by Cornie and Zhang [13].

The addition of carbon fibers is instrumental to control distributed fracture under dynamic conditions without sacrificing material strength. These composites can be also used as components in reactive materials, for example in mixture with Teflon [14,15].

2. Experimental techniques

Two composite materials were supplied by Metal Matrix Cast Composite, LLC. The C_{Pitch}/Al–Mg composite consists of a

* Corresponding author at: Department of Mechanical and Aerospace Engineering, University of California, San Diego, CA 92093, United States. Tel.: +1 858 534 4719; fax: +1 858 534 5698.
E-mail address: mameyers@ucsd.edu (M.A. Meyers).

0921-5093/$ – see front matter © 2007 Elsevier B.V. All rights reserved.
doi:10.1016/j.msea.2007.08.055

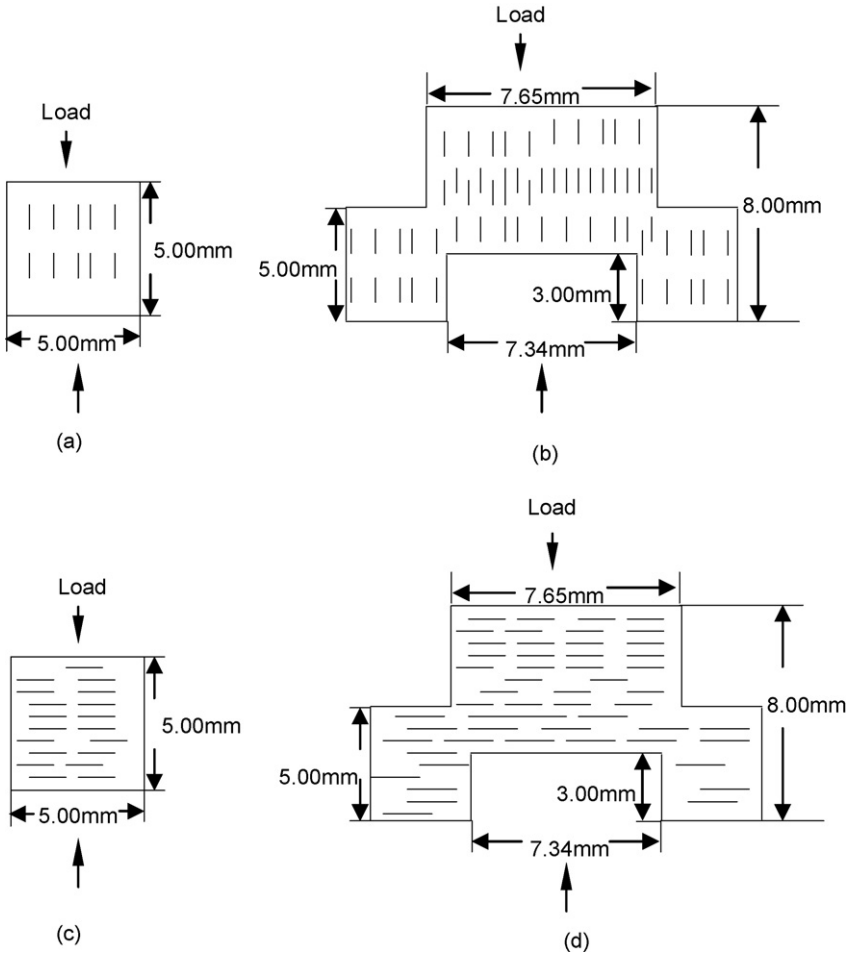

Fig. 1. Geometry of cylindrical and hat-shaped specimens: (a and b) fibers oriented parallel (||) to loading direction and (c and d) fibers perpendicular (⊥) to loading direction.

70 vol% metal matrix filled with 30 vol% pitch-based carbon fibers. The theoretical density is 2.47 g/cm^3. The density of the material is 2.43 g/cm^3 and porosity is 1.6%. The C_{PAN}/Al–Mg composite also consists of a 70 vol% metal matrix filled with 30 vol% PAN-based carbon fibers. The density of the material is 2.20 g/cm^3 and porosity is 10.9%. For reference purposes, tests were also run on the unfilled matrix material, Al–Mg, consisting of 90 wt% Al and 10 wt% Mg.

Milled pitch-based and milled PAN-based carbon fibers were used; these fibers were not chopped. The diameters of both types of fibers are 10 μm nominally. C_{Pitch} has a nominal length of 200 μm while C_{PAN} about 300 μm. C_{PAN} was produced from PAN fiber after carbonization. C_{Pitch} was produced from petroleum pitch after carbonization and then graphitization at an even higher temperature. C_{Pitch} usually has lower tensile and compressive strengths but a higher modulus than C_{PAN} [16]. There is no special treatment on the fibers to enhance the interfacial bonding between the metal matrix and fibers. The Al–Mg infiltration was performed at a temperature of about 750 °C. The specimens were machined in either a milling machine or a lathe via common Mg machining protocol without using any coolant.

Quasi-static compression tests were performed using Instron 3367 with a 30 kN loading capacity. Hopkinson bar compression tests [17,18] were used to investigate the high-strain rate compressive response of cylindrical specimens and the shear strength of hat-shaped specimens. Cylindrical specimens were tested at different strain rates (3000 s^{-1}, 5000 s^{-1}, 7000 s^{-1}).

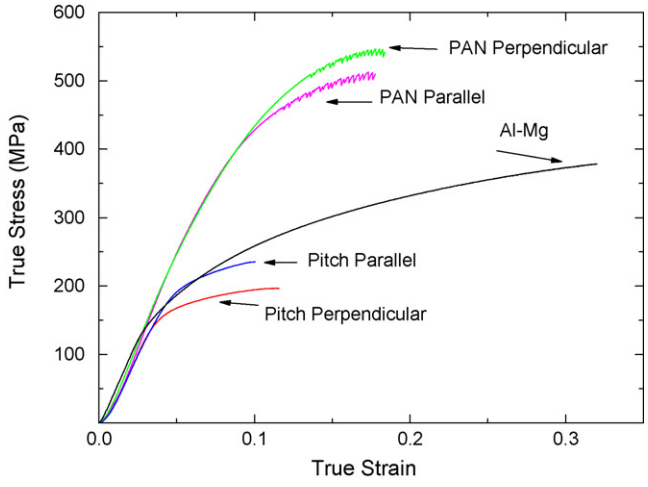

Fig. 2. Typical stress–strain curves of cylindrical specimens under quasi-static compression (~10^{-3} s^{-1}) for Al–Mg and two composites (PAN or pitch fibers parallel or perpendicular to loading).

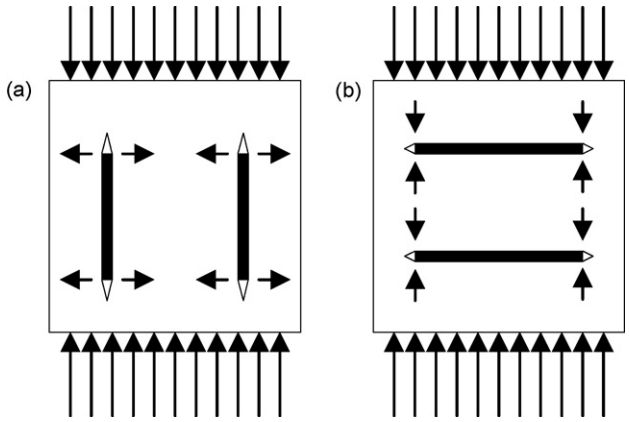

Fig. 3. Schematic drawing showing (a) opening of micro-cracks around fibers when parallel (||) to loading direction and (b) closing of micro-cracks around fibers when perpendicular (⊥) to loading direction.

The estimated shear strain rate for the hat-shaped specimen in dynamic tests is 35,000 s^{-1}. The geometry of the corresponding specimens is shown below in Fig. 1. Loading was carried out perpendicularly (⊥) or parallel (||) to carbon fibers. The parallel (||) and perpendicular (⊥) orientations are shown with the schematic fiber directions (Fig. 1).

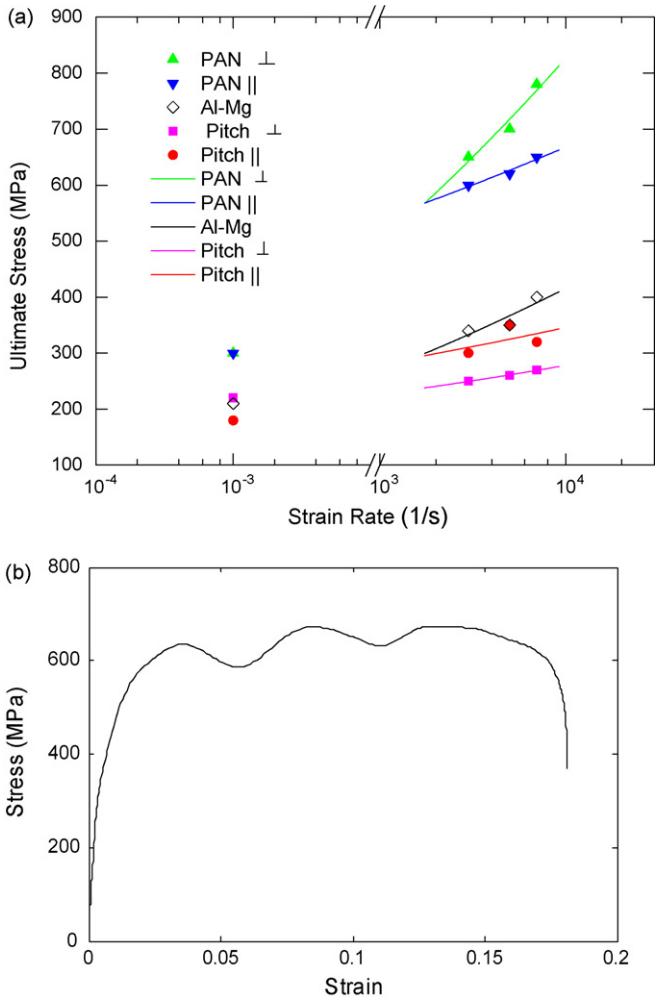

Fig. 4. (a) Experimental data (all symbols) and fitted curves (only for the data from high-strain rate deformation) of all materials and (b) stress–strain curve of a C_{PAN}/Al–Mg composite specimen at 7000 s^{-1} deformation.

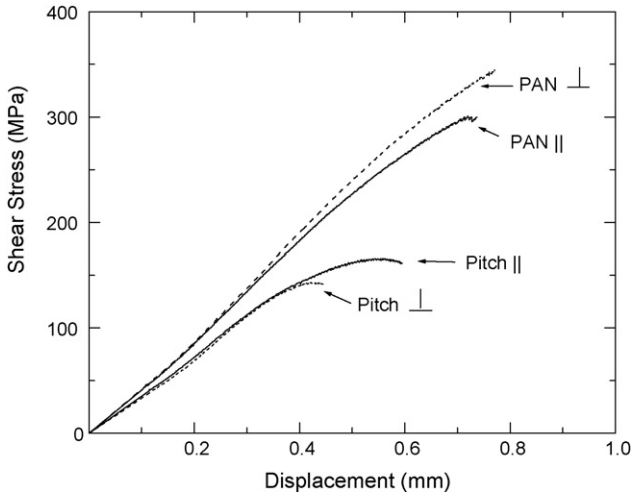

Fig. 5. Quasi-static compressive response of hat-shaped specimens of composite materials with different types and orientation of fibers.

3. Results and discussion

3.1. Compressive strength

The quasi-static stress–strain curves of materials are shown in Fig. 2. The C_{PAN}/Al–Mg (PAN ⊥ and PAN ||) has a higher compressive strength than C_{Pitch}/Al–Mg (Pitch ⊥ and Pitch ||). This response is consistent with the fact that PAN-based carbon fibers usually have a higher strength than pitch-based carbon fibers. The compressive strength of the metal matrix (Al–Mg) is higher than that of the C_{Pitch}/Al–Mg and lower than that of C_{PAN}/Al–Mg. Meanwhile, the metal matrix presents much higher strain at the fracture (~50%) than both composites (~10% and ~20%). This is due to (a) both pitch-based carbon fiber and PAN-based carbon fiber have much lower critical strains [19]; (b) the low interfacial strength between the fibers and the metal matrix; and (c) the generation of micro-cracks in the composite upon loading.

It is proposed that the change in elastic moduli with load in Fig. 2 is due to micro-cracks produced in the compression process. It is known (e.g. [20], [21]) that micro-cracks decrease the elastic modulus. The following expression was developed by O'Connell and Budiansky [21]:

$$E = E_0(1 - 1.63Na^3) = E_0(1 - 1.63D),$$

where N is the number of cracks per unit volume, a the radius of a mean crack, and $Na^3 = D$, where D is a damage parameter. Li et al. [22] applied this equation to a material in which the damage changes with strain, ε, as $D = D_0 + K\varepsilon^n$, where D_0 is the initial damage and n is a damage accumulation parameter. Therefore, the stress σ is obtained as follows:

$$\sigma = E_0\left[(1 - 1.63D)\varepsilon - \frac{1.63K\varepsilon^{n+1}}{n+1}\right].$$

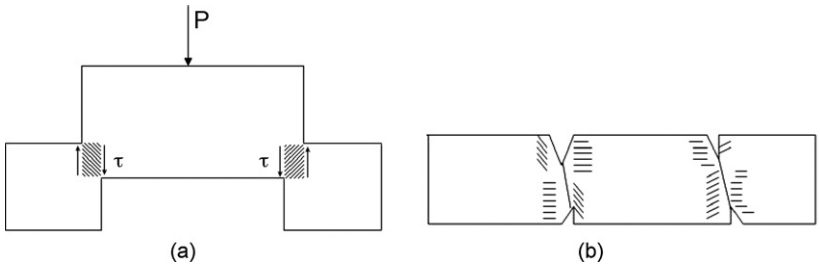

Fig. 6. (a) Schematic illustration of a hat-shaped specimen undergoing compression with shear zone shown by shaded areas and (b) schematic illustration of plastic flow of material filled with fibers in the sheared zone after testing.

It can be seen that this is a non-linear relationship between σ and ε. The second term in the above equation is negative and decreases the slope in a stress–strain curve. Thus, damage accumulation at the extremities of the fibers (Fig. 3) can lead to a concave curve and a decrease in modulus as shown in Fig. 2. This is an alternative explanation to work hardening of the metal matrix.

The results of Hopkinson bar compressive tests, consistent with the quasi-static results, are presented in Fig. 4. C_{PAN}/Al–Mg has a higher compressive strength than both C_{Pitch}/Al–Mg and the Al–Mg matrix. The dependence of compressive strength on strain rate can also be clearly seen in Fig. 4(a). A typical stress–strain curve is also presented in Fig. 4b. The higher the strain rate, the higher compressive strength for both materials. However, for "C_{Pitch} perpendicular" the compressive strength practically did not change with strain rates. Carbon fibers are usually strain rate insensitive [23], while the metal matrix (Al–Mg) is strain rate sensitive, as shown in Fig. 4. It can be concluded that the strain rate sensitivity of the composites is mainly caused by the strain rate sensitivity of the metal matrix. The strain rate dependence of the debonding process can also contribute to the global strength of composites.

3.2. Shear strength

Quasi-static tests (Fig. 5) of the hat-shaped specimens confirm that C_{PAN}/Al–Mg (PAN $\perp$ and PAN ||) has a higher shear strength than C_{Pitch}/Al–Mg (Pitch $\perp$ and Pitch ||). The result is consistent with the fact that PAN-based carbon fibers usually have a higher tensile and compressive strength than pitch-based carbon fibers. The orientation of fibers did not have a significant impact on the shear strength of composites.

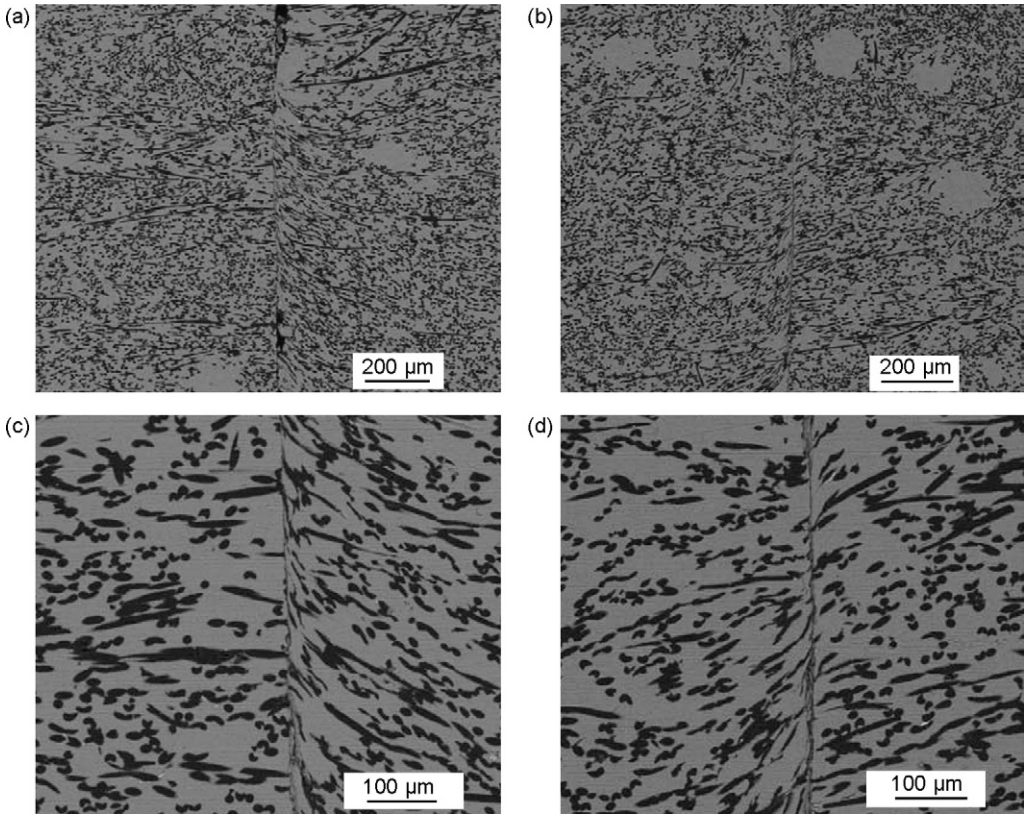

Fig. 7. SEM micrographs exhibiting the shear zone and plastic flow pattern in a C_{Pitch}/Al–Mg specimen: (a) low magnification of shear zone (left hand side of the sheared sample); (b) low magnification of shear zone (right hand side); (c) high magnification of shear zone (left hand side); (d) high magnification of shear zone (right hand side).

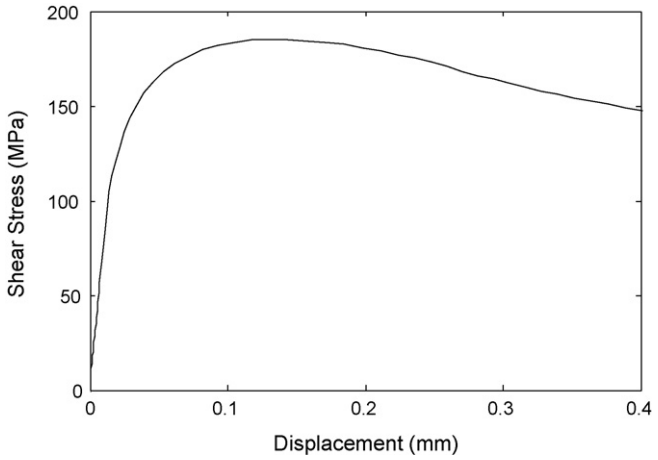

Fig. 8. Shear stress–displacement curve of a hat-shaped C_{Pitch}/Al–Mg specimen.

The shear strain and strain rate in the hat-shaped specimen can be estimated from the measured displacement as a function of measured time [24] and estimated thickness of the sheared region, in our case, using a SEM micrograph. The schematic shear zones and plastic flow are illustrated in Fig. 6. The average strain rate in the hat-shaped specimens is calculated from the velocity of the incident bar, v, divided by the thickness of the plastic deformation region, t:$\dot{\gamma} = v/t$. The velocity of the incident bar was 7 m/s. The thickness of the sheared region was measured from SEM micrograph of the specimen and is roughly equal to ~200 μm (Fig. 7). Therefore, the strain rate is:

$$\dot{\gamma} = \frac{v}{t} = \frac{7}{200 \times 10^{-6}} = 3.5 \times 10^4\ \mathrm{s}^{-1}$$

The stress state in the deformed region is fairly close to simple shear and the strain is approximately equal to the ratio between the critical shear displacement d (Fig. 8) and the thickness of the deformed region, t (Fig. 6):

$$\gamma = \frac{d}{t} = \frac{0.15}{0.2} = 0.75.$$

Table 1 shows that the maximum average shear strength of composite specimens did not depend significantly on fiber orientation (perpendicular and parallel to loading direction) for both the pitch-based carbon fibers and the PAN-based carbon fibers. The maximum average shear strength of C_{PAN}/Al–Mg (400 MPa) is almost twice that of C_{Pitch}/Al–Mg (220 MPa) for both (perpendicular or ||) orientations of the fibers. As noted above, this phenomenon is consistent with the fact that PAN-based carbon fibers usually are stronger than pitch-based carbon fibers. There is a tendency to higher critical displacements for specimens filled with PAN-based carbon fibers probably because the PAN-based carbon fibers have a higher tensile strength than pitch-based carbon fibers. By contrast, the shear strength of the metal matrix is higher than those of C_{Pitch}/Al–Mg but lower than those of C_{PAN}/Al–Mg. The critical displacement of the metal matrix specimens is much larger than those of carbon fiber filled composites, because the carbon fibers are more brittle than the metal matrix. It means that Al-based composites filled with fibers may combine high shear strength and low critical shear strain, which may enhance bulk-distributed fracture at impact.

3.3. Microstructures

The microstructure of the hat-shaped specimens of C_{Pitch}/Al–Mg (fibers placed parallel to loading direction) is presented in Fig. 9. It reveals that the failure mechanism of the specimen includes both fracture and pull-out of fibers (arrows in the Fig. 9a). The characteristics of the fibers fracture in the present C_{Pitch}/Al–Mg are similar to those in the high-modulus fiber/AM20-matrix composite [5], showing single-fiber fracture.

The behavior of pitch fibers placed perpendicular to loading direction inside the shear zone under high-strain rate deformation is shown in Fig. 10. Compared to the fibers parallel to loading direction, they were heavily bent. Fracture of the fibers related to the area of local tensile strains due to bending is noticeable (Fig. 10a). Fibers are also split or comminuted in the bending zone (Fig. 10b). The sheet-like structure of the cross-section of pitch fibers in Fig. 9b could explain why the composites filled with perpendicular pitch fibers have a lower compressive strength than the ones with parallel pitch fibers.

Based on high-resolution SEM imaging, Vezie and Adam [16] observed that high-compressive strength PAN fibers usually had rough, granular textures and pitch fibers had a sheet-like structure, which contributed to the low-compressive strength of pitch fibers. SEM micrographs of PAN fibers in our specimens (Fig. 11b) also display such texture. The rough surface of the fibers could facilitate force transfer and lead to high strength of the composites. Compared to the failure mechanism of pitch fibers in the composite, the main reason attributed to the failure of PAN fibers is cracking (inside the circles, Fig. 11a). Fig. 12 shows that cracks also propagated along the interface between the metal matrix and carbon fibers.

PAN fibers seemed to be uniformly distributed in the undeformed part of a specimen (Fig. 13a). However, a locally high

Table 1
Maximum shear strength and critical displacements for dynamic hat-shaped specimen tests

Composite type	Fiber orientation to loading direction	Average maximum shear strength (MPa)	Average critical displacement (μm)
Pitch fiber filled Al–Mg alloy	⊥	220	100
	||	220	200
PAN fiber filled Al–Mg alloy	⊥	390	280
	||	400	320
Al–Mg alloy (no fiber)		280	600

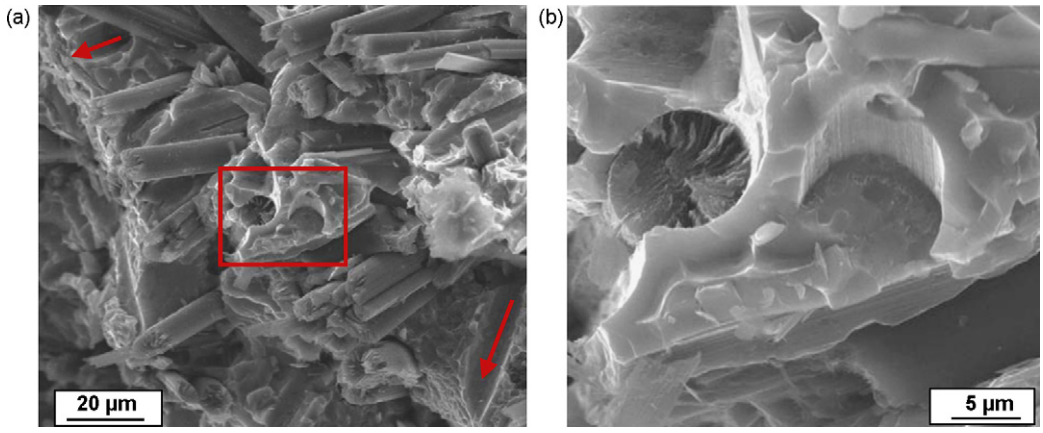

Fig. 9. Microstructure of a hat-shaped C_{Pitch}/Al–Mg specimen (fibers parallel to loading direction): (a) low magnification fracture and pull-out (indicated by arrows) of fibers and (b) high magnification shows fractured fibers.

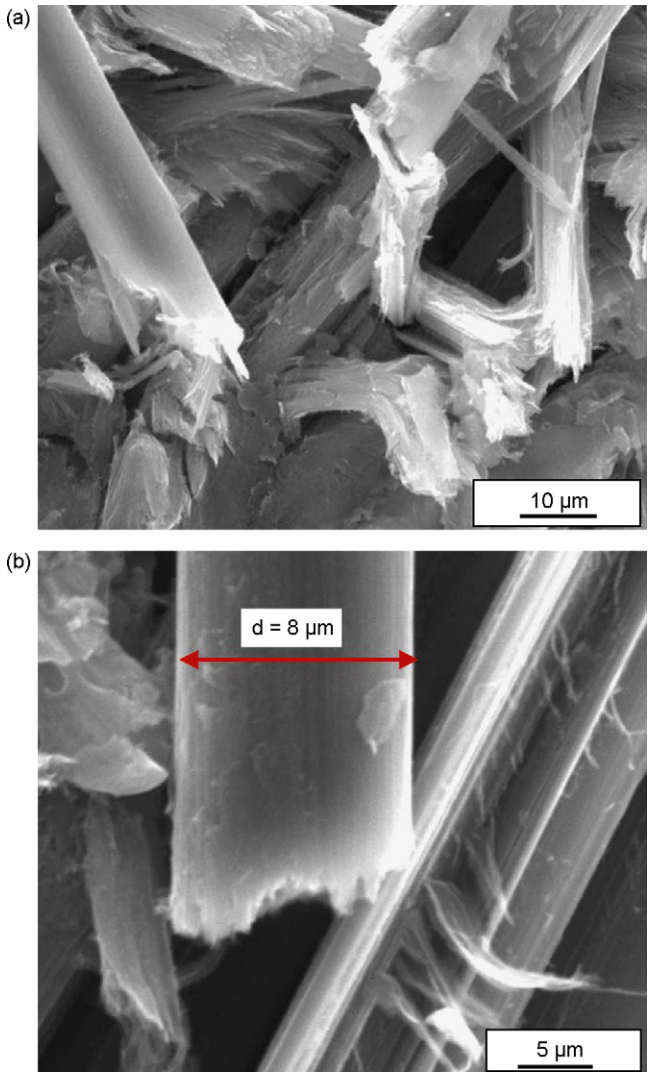

Fig. 10. SEM micrograph of a C_{Pitch}/Al–Mg specimen (fibers perpendicular to loading direction) showing (a) bent and fractured fibers and (b) a split carbon fiber.

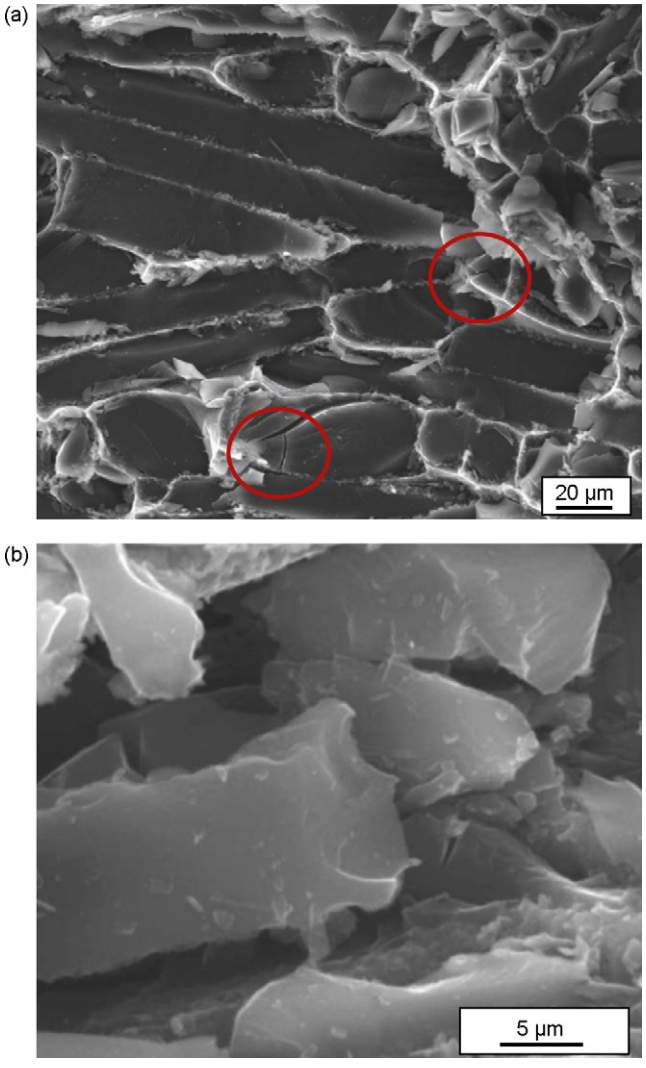

Fig. 11. Micrographs of fractured PAN-based carbon fibers in C_{PAN}/Al–Mg specimens (fibers parallel to loading direction) show (a) cracks of fibers and (b) rough and granular texture of fibers.

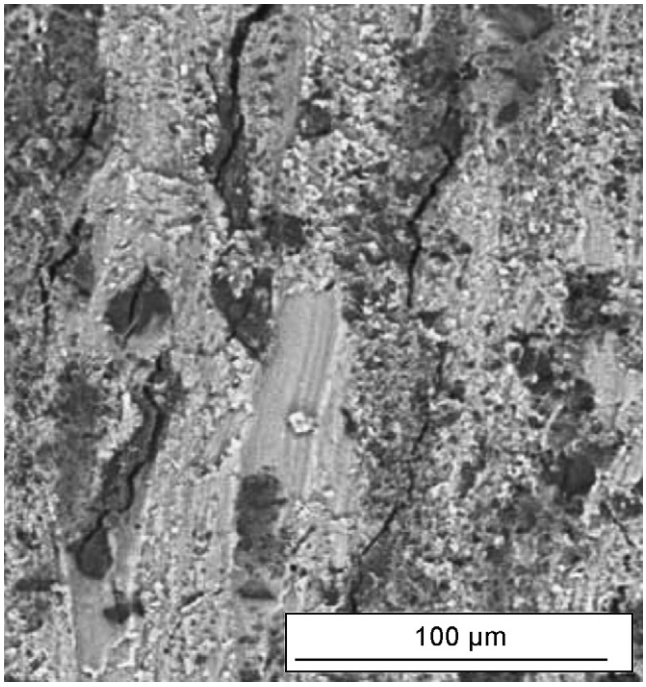

Fig. 12. SEM micrograph showing cracks in the fracture surface of a C_{PAN}/Al–Mg specimen (fibers perpendicular to loading direction).

concentration of fibers (Fig. 13b) in the ring part of the specimen is shown. It can be speculated that the fracture of this part due to tensile stress tended to happen in the high concentration region of carbon fibers. It shows good agreement with one of research goals, which is to use fibers to facilitate bulk-distributed fracture (fragmentation) of the composites.

3.4. Fracture characterization

We observed a broad distribution of values of critical strains, which did not depend on strain rate, the nature of fibers or their orientation.

Specimens were fractured mainly by macroshear in combination with bulk-distributed damage. At high strain rates, the cylindrical specimens were comminuted into a large number of small pieces. For the same strain rate, C_{Pitch}/Al–Mg specimens tended to be fragmented into more pieces than C_{PAN}/Al–Mg specimens. This demonstrates that the fracture patterns are influenced by the nature of carbon fibers. Such different fragmentation could also be related to the different porosity of the composites. The weaker pitch-based carbon fibers facilitate bulk-distributed fracture, resulting in smaller size of fragments. This mode of fracture can be beneficial when this alloy is used as the metallic component in reactive materials.

Another interesting observation of the fragmented cylindrical specimens after high-strain rate deformation is the existence of some reddish fragmentation products (circles in Fig. 14) among regular black pieces after tests. Such phenomenon was observed for specimens at 5000 s^{-1} or 7000 s^{-1} deformation regardless of the type or the orientation of carbon fibers, but not for any specimens under 3000 s^{-1} deformation. The difference in mechanical

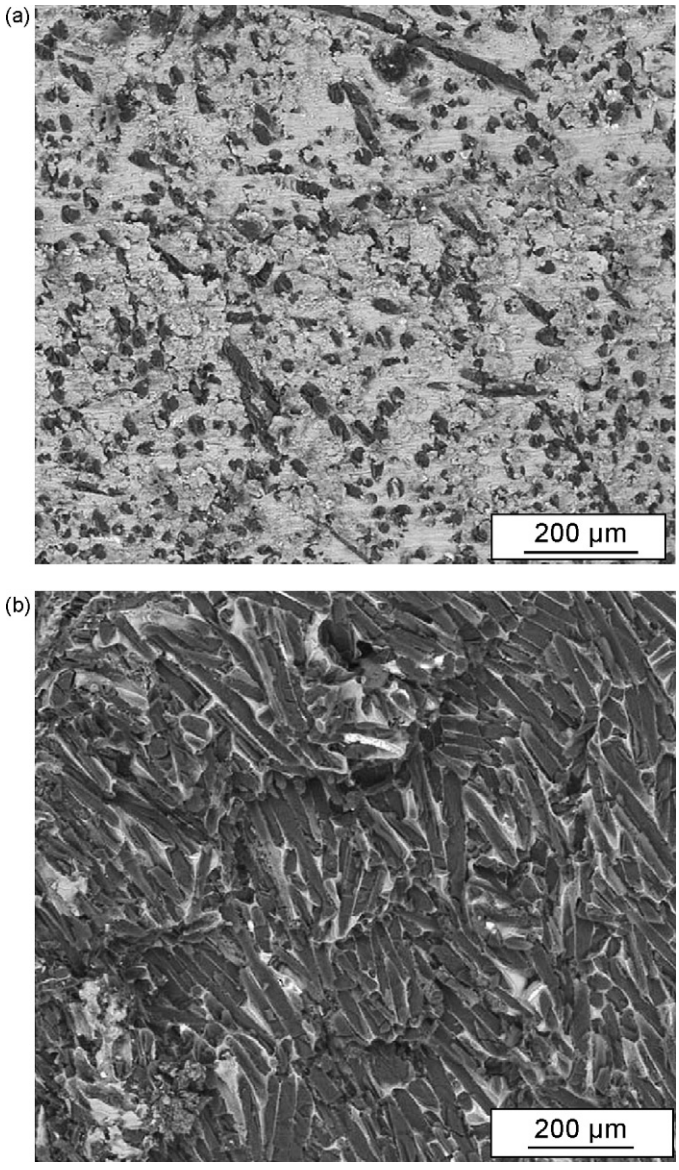

Fig. 13. SEM micrographs of the fractured ring part of a C_{PAN}/Al–Mg specimen (fibers perpendicular to loading direction): (a) low magnification of the external surface of undeformed specimen showing fibers distributed uniformly and (b) fracture surface in the region where the volume fraction of fibers (dark rods) is much higher than 30%.

Fig. 14. Reddish fragments (typical size about 1 mm) observed among regular black scattered pieces after dynamic testing and comminution of C_{Pitch}/Al–Mg specimen bulk damaged at high-strain rate (5000 s^{-1} or 7000 s^{-1}). (For interpretation of the references to color in this figure legend, the reader is referred to the web version of the article.)

behavior for specimens under different deformation conditions may affect energy dissipation, resulting in different input to their chemical reaction. It may be concluded that these materials are inert under low-strain rate deformation, but need a significant amount of mechanical work, for example under high-strain rate plastic deformation, to drive the reaction [25]. It is obvious that further work is warranted in order to determine the products of the possible reactions between Al and carbon fibers [26,27] and between magnesium and carbon fibers [28] are desirable.

The dynamic critical tensile strains for opening of macro-cracks can be estimated from the hat-shaped specimens based on the diameters of the hat part and of the hole. During the movement of the hat (with larger diameter: 7.65 mm) into the hole (smaller diameter: 7.34 mm) the maximum tensile (hoop) strains can be computed and are about 4%. The external ring fractured at this hoop strain. Thus, this value is an upper estimate for tensile strain for opening macro-cracks, because a crack could open at an intermediate stage of the penetration process of the hat part into the hole.

Metal matrix specimens were deformed without developing shear macro-cracking upto large values of compressive strain. This means that filling with fibers facilitates shear fracture at earlier stages of deformation irrespective of the strain rate. This can be beneficial for the initiation of the reaction between Al and carbon fibers and between Mg and carbon fibers to form Al_4C_3 [26,27] or Mg_2C_3 and MgC_2 [29] during fracture under dynamic compression.

4. Conclusions

High-strain rate testing was performed on carbon fiber (PAN or pitch) filled Al–Mg metal matrix composites. The PAN-based composite was much stronger in compression than the associated material made with pitch fibers. Experiments and analysis on the effect of the type and orientation of carbon fibers on the mechanical properties of the composites lead to the following conclusions:

(a) Quasi-static compression tests and dynamic Hopkinson bar tests demonstrated that the compressive strength of composite specimens does depend significantly on strain rate regardless of fiber orientation (perpendicularly or parallel to the loading direction) for C_{PAN}/Al–Mg and C_{Pitch}/Al–Mg. The compressive strength of composites increased with increasing strain rate mainly because of the strain rate sensitivity of the metal matrix.

(b) Compressive strength and maximum average shear strength of C_{PAN}/Al–Mg specimens are almost twice that of C_{Pitch}/Al–Mg for both orientations of the fibers. This effect is consistent with the fact that PAN-based carbon fibers usually have higher compressive and tensile strength than pitch-based carbon fibers.

(c) The presence of fibers reduced the critical strain for fracture for both composites and enhanced bulk-distributed fracture (fragmentation) under dynamic compressive and shear deformation.

(d) The microstructure of hat-shaped specimens after high-strain rate shear deformation reveals that fracture and pull-out of fibers were the major failure mechanisms of the C_{Pitch}/Al–Mg with fibers parallel to loading direction. Bending and splitting of fibers were the major failure mechanisms of the C_{Pitch}/Al–Mg with fibers perpendicular to loading direction. Cracking of fibers and cracks along the interface between the metal matrix and carbon fibers were the major failure mechanism of the C_{PAN}/Al–Mg.

(e) A possible reaction of the metal matrix with carbon fibers led to the unusual reddish scattered pieces in the fragmented cylindrical specimens under high-strain rate compressive deformation ($5000\,s^{-1}$ or $7000\,s^{-1}$). Further investigation on it is necessary.

Acknowledgements

We thank the US Office of Naval Research MURI ONR Award N00014-07-1-0740 (Dr. J. Goldwasser, Program Director) and the SBIR Program of Defense Threat Reduction Agency HDTRA1-05-P-0142 (Dr. Kibong Kim, Program Sponsor) for support of the research program. Scanning electron microscopy was carried out with the assistance of Evelyn York (SIO). Her help is greatly appreciated.

References

[1] I.W. Hall, Metallography 20 (1987) 237–246.
[2] J.W. Kaczmar, K. Pietrzak, W. Wlosinski, J. Mater. Process. Technol. 106 (2000) 58–67.
[3] T. Kuzumaki, O. Ujiie, H. Ichinose, K. Ito, Adv. Eng. Mater. 2 (2000) 416–418.
[4] A. Mortensen, I. Jin, Int. Mater. Rev. 37 (1992) 101–128.
[5] A. Feldhoff, E. Pippel, J. Woltersdorf, Adv. Eng. Mater. 2 (2000) 471–480.
[6] M. Lancin, C. Marhic, J. Eur. Ceram. Soc. 20 (2000) 1493–1503.
[7] M.H. Vidal-Setif, M. Lancin, C. Marhic, R. Valle, J.-H. Raviart, J.-C. Daux, M. Rabinovitch, Mater. Sci. Eng. A 272 (1999) 321–333.
[8] J. Bijwe, R. Rattan, M. Fahim, Tribol. Int. 40 (2007) 844–854.
[9] Y.Z. Wan, Y.L. Wang, H.L. Luo, G.X. Cheng, K.D. Yao, J. Appl. Polym. Sci. 75 (2000) 987–993.
[10] P. Soroushian, M. Nagi, A. Okwuegbu, ACI Mater. J. 89 (1992) 491–494.
[11] C.C. Poteet, I.W. Hall, Mater. Sci. Eng. A A222 (1997) 35–44.
[12] Y. Zhou, Y. Wang, S. Jeelani, Y. Xia, Appl. Compos. Mater. 14 (2007) 17–31.
[13] J.A. Cornie, S. Zhang, SPIE Proc. Ser. 5288 (2003) 310–315.
[14] A.Y. Dolgoborodov, M.N. Makhov, I.V. Kolbanev, A.N. Streletskii, V.E. Fortov, JETP Lett. 81 (2005) 311–314.
[15] A.A. Denisaev, A.S. Shteinberg, A.A. Berlin, Doklady Phys. Chem. 414 (2007) 139–142.
[16] D.L. Vezie, W.W. Adams, J. Mater. Sci. Lett. 9 (1990) 883–887.
[17] H. Kolsky, Proceedings of the Physical Society Section B, vol. 62, 1949, pp. 676–700.
[18] L.W. Meyer, S. Manwaring, in: L.E. Murr, K.P. Staudhammer, M.A. Meyers (Eds.), Metallurgical Application of Shock-Wave and High-Strain-Rate Phenomena, Marcel Dekker, New York, 1986, pp. 657–674.
[19] T. Ohsawa, M. Miwa, M. Kawade, E. Tsushima, J. Appl. Polym. Sci. 39 (1990) 1733–1743.
[20] R.L. Salganik, Izvestiya Akademii Nauk, S.S.S.R., Mekhanika Tverdogo Tela 8 (1973) 149–158.
[21] R.J. O'Connell, B. Budiansky, J. Geophys. Res. 79 (1974) 5412–5426.
[22] T. Li, F. Jiang, E.A. Olevsky, K.S. Vecchio, M.A. Meyers, Mater. Sci. Eng. A 443 (2007) 1–15.
[23] Y.X. Zhou, D.Z. Jiang, Y.M. Xia, J. Mater. Sci. 36 (2001) 919–922.

[24] M.A. Meyers, G. Subhash, B.K. Kad, L. Prasad, Mech. Mater. 17 (1994) 175–193.
[25] R.G. Ames, Mater. Res. Soc. Symp. Proc. 896 (2006) 123–132.
[26] R.T. Pepper, R.A. Penty, J. Compos. Mater. 8 (1974) 29–37.
[27] P.W. Jackson, Met. Eng. Q. 9 (1969) 22–30.
[28] S.I. Dement'ev, A.A. Zabolotskii, I.V. Romanovich, S.A. Prokof'ev, S.E. Salibekov, Soviet Powder Metall. Met. Ceram. 16 (1977) 197–200.
[29] M. Hansen, K.P. Anderko, Constitution of Binary Alloys, Genium Publishing Co., 1989.